1   **Projected Increases in North Atlantic Tropical Cyclone**
2   **Intensity from CMIP5 Models**
3

4   Gabriele Villarini[1], and Gabriel A. Vecchi[2]
5
6
7   [1] IIHR-Hydroscience & Engineering, The University of Iowa, Iowa City, Iowa
8
9   [2] Geophysical Fluid Dynamics Laboratory, National Oceanic and Atmospheric
10   Administration, Princeton, New Jersey
11

16
17
18

19   *Corresponding author address:*
20   Gabriele Villarini, IIHR-Hydroscience & Engineering, The University of Iowa, Iowa
21   City, IA 52242. E-mail: gabriele-villarini@uiowa.edu
22

1   ABSTRACT

2

3   Tropical cyclones – particularly intense ones – are a hazard to life and property, so an

4   assessment of the changes in North Atlantic tropical cyclone intensity has important

5   socio-economic implications. In this study we focus on the seasonally integrated Power

6   Dissipation Index (PDI) as a metric to project changes in tropical cyclone intensity.

7   Based on a recently developed statistical model, we examine projections in North

8   Atlantic PDI using output from 17 state-of-the-art global climate models and three

9   radiative forcing scenarios. Overall, we find that North Atlantic PDI is projected to

10   increase with respect to the 1986-2005 period across all scenarios. The difference

11   between the PDI projections and those of the number of North Atlantic tropical cyclones,

12   which are not projected to increase significantly, indicates an intensification of North

13   Atlantic tropical cyclones in response to both greenhouse gas (GHG) increases and

14   aerosol changes over the current century. At the end of the 21st century, the magnitude of

15   these increases shows a positive dependence on projected GHG forcing. The projected

16   intensification is significantly enhanced by non-GHG (primarily aerosol) forcing in the

17   first half of the 21st century.

18

19

1. Introduction

The projected damage arising from tropical cyclones is in a future climate, particularly as anthropogenic global warming continues, is a topic of scientific and societal interest, and will be influenced by changes in storm intensity, population and vulnerability (*e.g.*, Mendelsohn *et al.* 2012, Peduzzi *et al.* 2012). The most intense hurricanes (Cat 3-5) are responsible for the vast majority of the tropical cyclone damage in the United States, even though they represent only one fourth of the overall landfalling tropical cyclone activity (*e.g.*, Pielke *et al.* 2008).

Theoretical considerations (*e.g.*, Emanuel 1987, Holland 1997) and high-resolution modeling studies (*e.g.*, Knutson and Tuleya 2004, Oouchi *et al.* 2006, Emanuel *et al.* 2008, Bender *et al.* 2010, Knutson *et al.* 2010) generally suggest an increase in the intensity of tropical cyclones in a warming climate. High-resolution models can represent the most intense storms directly, but the required computational expense generally limits them to single-model runs and/or time slice experiments. At the present time, it is unclear what outcome we would get by running these high-resolution models in a multi-model fashion over the entire 21st century.

An alternative approach to counting the number of the most intense storms is to employ the seasonally integrated Power Dissipation Index (PDI; Emanuel 2005, 2007), which is a metric that convolves storm duration, frequency, and intensity. Storm intensity is accounted for by taking the third power of the wind speed. Emanuel (2005) found that there was a high correlation between PDI and tropical Atlantic sea surface temperature (SST). Swanson (2008) obtained a higher correlation using the difference between tropical Atlantic (SST$_{Atl}$) and tropical mean SSTs (SST$_{Trop}$). Vecchi *et al.* (2008b)

1 showed that projections of PDI based on relative SST (the difference between SST_{Atl} and

2 SST_{trop}) are in better agreement with results from dynamical models than using SST_{Atl}

3 alone. Recently, Villarini and Vecchi (2012a) developed a statistical model in which

4 SST_{Atl} and SST_{Trop} are used as predictors (see Section 2). We have also recently shown

5 that this statistical model can be used to make retrospective skillful forecasts of

6 seasonally integrated North Atlantic PDI from November of the previous season,

7 allowing the skillful forecast of the upcoming season as the current one is still coming to

8 an end (Villarini and Vecchi 2012c).

9   Here we apply the model of Villarini and Vecchi (2012a) to outputs from 17 global

10 climate models (GCMs) produced under the Fifth Coupled Model Intercomparison

11 Project (CMIP5; Taylor et al. 2012; Table 1) to address questions related to future

12 changes in North Atlantic tropical cyclone intensity.

13 **2. Methodology**

14   The methodology used to create the projected North Atlantic PDI time series is based

15 on the model described in Villarini and Vecchi (2012a). Here we provide only a brief

16 overview and point the interested reader to the original reference for a more in-depth

17 discussion. The PDI record can be modeled according to a gamma distribution:

18
$$f_Y(y \mid \mu, \sigma) = \frac{1}{\left(\sigma^2 \mu\right)^{1/\sigma^2}} \frac{y^{-1+1/\sigma^2} \exp\left[-y/\left(\sigma^2 \mu\right)\right]}{\Gamma\left(1/\sigma^2\right)} \tag{1}$$

19 in which the logarithm of the location parameter μ is a linear function of SST_{Atl} and

20 SST_{Trop}:

21
$$\log(\mu) = 0.76 + 1.94 \cdot SST_{Atl} - 1.78 \cdot SST_{Trop} \tag{2}$$

1   and *log(σ)* is constant and equal to -0.57. The calculations are performed in R (R

2   Development Core Team 2008) using the freely available GAMLSS package

3   (Stasinopoulos *et al.* 2007).

4   This parsimonious model can describe very well the interannual and decadal

5   variability and change of the PDI record over the period 1949-2008 (compare red and

6   blue lines in Fig. 1; Villarini and Vecchi 2012a), and allows for century-scale

7   reconstructions of PDI (yellow line Fig. 1).

8   The statistical frameworks modeling Atlantic hurricane activity using SST_{Atl} relative

9   to SST_{Trop}, rather than SST_{Atl} alone, are supported by both modeling and empirical results

10   (*e.g.*, Latif *et al.* 2007, Vecchi and Soden 2007a, Swanson 2008, Bender *et al.* 2010, Zhao

11   *et al.* 2010, Ramsay and Sobel 2011, Vecchi *et al.* 2008b, 2011, Villarini *et al.* 2010,

12   2011, 2012) and are the basis of skillful seasonal forecasts (Vecchi *et al.* 2011, Zhao *et*

13   *al.* 2010, Villarini and Vecchi 2012c). In the model of Villarini and Vecchi (2012a), the

14   positive coefficient on Atlantic SSTs is larger than the negative coefficient on tropical-

15   mean SSTs (equation 2), and a similar difference in the magnitude of the Atlantic and

16   tropical-mean coefficients to the fit of PDI was found by Swanson (2008). This indicates

17   that uniform warming (cooling) of the tropics should lead to an increase (decrease) in

18   PDI. In addition, warming (cooling) of the Atlantic relative to the tropical average will

19   also lead to an increase (decrease) in PDI.

20   In this study we examine projected changes in PDI by applying the statistical model

21   of Villarini and Vecchi (2012a) to outputs from 17 GCMs (see Table 1 for a list) to

22   address questions related to future changes in North Atlantic tropical cyclone intensity,

23   using 1986-2005 as our reference period to compute anomalies, and the median of the

5

1 gamma distribution as reference value. We have recently analyzed these GCMs for

2 possible changes in tropical cyclone activity (Villarini and Vecchi 2012b). We showed

3 that over the first half of the 21st century there is a significant radiatively forced increase

4 in North Atlantic tropical storm frequency, which is not driven by CO_2 but likely

5 aerosols. This increase, however, does not extend over the entire 21st century, for which

6 the sign of the trend is uncertain. Differences in the behavior of PDI and tropical cyclone

7 frequency indicate changes in tropical cyclone intensity and duration at the strongest

8 intensities (Villarini and Vecchi 2012a).

9 **3. Results**

10 Figure 1 shows the time series of PDI anomalies for three representative

11 concentration pathways (RCPs; each RCP is labeled to reflect the radiative forcing

12 change at the end of the 21st century, in W/m^2). The observations over the period 1949-

13 2008 are within the GCMs ensemble spread. The projected PDI values tend to be larger

14 than the PDI values over the last 130 years. Regardless of the RCP, there is a tendency

15 towards increases in PDI over the 21st century. The magnitude of these increases depends

16 on the RCP, with RCP 2.6 showing smaller increases compared to RCP 8.5. This

17 magnitude increase is coupled with an increase in the ensemble spread (Figures 1-2). The

18 projected mean over 2016-2035 is, on average, 20% larger than the corresponding values

19 over 1986-2005 (Figure 2). Averaged over 2046-2065, the multi-model mean PDI values

20 are between 50% and 75% larger than the values for the reference period. At the end of

21 the 21st century, the magnitude of the changes shows a positive dependence on the

22 strength of projected greenhouse gas (GHG) forcing.

1   With the exception of RCP 2.6, which has a mid-century maximum in GHG forcing,

2   the largest projected increases in PDI are towards the end of the 21st century. For RCP 4.5

3   (approximately a CO_2 doubling at the end of the 21st century) the PDI values over 2080-

4   2099 are on average 50% larger than the reference period. Meanwhile, the PDI values for

5   RCP 8.5 (approximately a quadrupling of CO_2 at the end of the 21st century) are, on

6   average, 100% larger than over 1986-2005, with a large increase in intermodel

7   variability.

8   Storm duration, frequency and intensity are used to compute the PDI. Could it be that

9   the increases in PDI are reflecting an increase in tropical cyclone frequency? A recent

10   analysis of the same GCMs (Villarini and Vecchi 2012b) showed that the ensemble-mean

11   North Atlantic tropical cyclone frequency is not projected to change significantly over the

12   entire 21st century, regardless of the RCP. In further contrast to the PDI projections,

13   frequency increases that were found were the largest in the first half of the 21st century

14   (driven by aerosol changes) and showed no relation to GHG forcing. The increase in PDI,

15   therefore, indicates a projection for an increase in North Atlantic tropical cyclone

16   intensity or the duration over which these storms are at their strongest intensities. A

17   scaling argument in Villarini and Vecchi (2012a) suggests that these projections include

18   an increase in the time during which North Atlantic tropical cyclones are at their

19   strongest intensities; that is, all other things equal, the probability of a major hurricane

20   occupying a place at any given time is projected to increase. In indicating that North

21   Atlantic tropical cyclone frequency and intensity can behave disparately, these results

22   using the CMIP5 GCMs are qualitatively consistent with previous analyses using the

previous third Coupled Model Intercomparison Project (CMIP3) models (Emanuel *et al.*
2008, Bender *et al.* 2010).

Multiple forcing agents (GHG, aerosols, ozone, etc.) are changing in these RCPs. An idealized suite of experiments in which CO_2 concentrations are doubled over a 70-year period isolates the impact of CO_2 in the projections (Figure 3). An increase in CO_2 results in an average slight increase in PDI, driven by the overall warming of the tropics (Villarini and Vecchi 2012a), in contrast to a CO_2-driven decrease found for tropical storm frequency (Villarini and Vecchi 2012b). However the magnitude of the PDI sensitivity to CO_2 in these models is not large enough to explain the increase in PDI for the three RCPs (e.g., compare the response at year 70 of Figure 3 with 2100 in RCP 4.5 of Figure 1), indicating that other forcing agents also contribute to the projected intensity increases.

To assess the role of aerosols in the PDI projections, we explore a partial perturbation experiment using a GCM from the CMIP5 suite (GFDL-CM3), in which aerosol precursors in RCP 4.5 are not allowed to change after 2005 and compare that to the response of the same model to the full RCP 4.5 projected forcing (Figure 4). This set of experiments indicates that the projected increase in PDI in the projections from GFDL-CM3 is driven both by GHG increases and aerosol changes (largely through a projected decrease in Atlantic and global aerosols; Villarini and Vecchi 2012b). The aerosol-driven increase in North Atlantic TC intensity in the GFDL-CM3 projections arises both from the tropical-mean warming driven by aerosol optical depth decreases, and from a warming of the Atlantic relative to the tropics driven by a more rapid reduction of aerosols over the Atlantic than over the global tropics in this RCP scenario.

1   Unfortunately, this experiment is not available for the full CMIP5 model suite; because of

2   the large potential role of aerosols in climate changes future coordinated experiments

3   should include idealized experiments like these to allow an assessment of the relative

4   contributions of aerosols and GHGs to projected climate changes.

5   An analysis of a couplet of historical CMIP5 experiments over the 1880-2005 period,

6   one using "all forcings" (changing GHGs, aerosols, natural forcing, etc.) and another

7   using past greenhouse forcing only (in which aerosols, natural forcings, etc. are kept at

8   preindustrial values) indicates that the projected influence of aerosol changes on PDI may

9   have begun in the 1990s (Figure 5). These historical perturbation experiments are only

10   available for a subset of the CMIP5 models (Table 1). In particular, the impact of GHGs

11   alone leads to an increase in PDI over the 20th century in these models, while the non-

12   GHG forcing leads to a decrease between the 1960s and 1980s, and a rebound following

13   that. Unfortunately again, experiments isolating the role of aerosols are available from

14   few CMIP5 models at this time; however, the timing of the non-GHG decrease suggests

15   that increasing aerosol loading in the Atlantic was a key countervailing force against a

16   GHG-induced increase of PDI over the 20th century, but over the recent decades (and in

17   the projections of the 21st century – see Figure 4) GHG and aerosol forcing both act to

18   increase PDI in these models.

19   **4. Discussion and Conclusions**

20   In this study we used output from a new suite of coupled climate simulations

21   (CMIP5; Taylor *et al.* 2005) and a recently developed statistical model (Villarini and

22   Vecchi 2012a) to project changes in North Atlantic PDI over the 21st century. These

23   analyses are based on 17 GCMs and explore three future radiative forcing scenarios (or

1   RCPs). Comparison of the PDI projections to projections of North Atlantic TC frequency

2   (Villarini and Vecchi 2012b) allows us to interpret the changes in terms of tropical

3   cyclone intensity. Our results suggest that the North Atlantic PDI, driven primarily by

4   changes to tropical cyclone intensity and the duration of TCs at highest intensity, is

5   projected to increase over the current century in all three RCPs. By the end of the 21st

6   century, the magnitude of the projected increase depends on the projected GHG forcing.

7   The a projected intensification of North Atlantic tropical cyclone in response to GHGs

8   increases and aerosol changes.

9   The results of this study are based on the statistical model described in Villarini and

10   Vecchi (2012a), in which the dominance of certain physical processes is implicit. In

11   particular, the model assumes that tropical tropospheric warming will follow something

12   close to a "moist adiabat" (warming will be about twice as large in the upper troposphere

13   than at the surface) and that the "weak temperature gradient" (WTG) approximation

14   holds (Sobel et al. 2002; the WTG approximation reflects the tendency of tropospheric

15   temperature anomalies to be relatively spatially homogeneous in the tropics). Therefore,

16   we do not account for the impact of direct radiative heating on free-atmospheric

17   temperatures (Emanuel 2010), which would require other relevant predictors that are

18   currently not included in the model. With these caveats in mind, these results point to a

19   substantial increase in North Atlantic tropical cyclone intensity, and growing probability

20   of extreme hurricane seasons over this century (Figure 6).

21   The CMIP5 coupled GCM experiment suite leads to a projection of increases in

22   North Atlantic PDI over the 21st century in response to projected increases in GHGs and

23   changes in atmospheric aerosols (largely reductions in Atlantic aerosol loading). The

1   projections for increased PDI reflect a projection of increase tropical cyclone intensity

2   and duration at the highest intensities, rather than an increase in frequency. These

3   projected changes in PDI are large, indicating substantially increased probability of years

4   as or more active than 2005 (Figure 6), which may have been the most active year on

5   record. However, these same models do not indicate that we should have seen an increase

6   over the past century – nor do reconstructions of PDI from SST (Figure 1; Villarini and

7   Vecchi 2012a). The lack of an expectation for increasing PDI over the past century in

8   these GCMs appears to arise in part because of large internal variability (Figure 1), but

9   also because the slight GHG-driven increase over the past century has been masked by a

10   sharp non-GHG driven decrease around the 1960s-1980s – the timing of which suggests a

11   role for aerosols (Figure 5), similar to a potential masking of a GHG-induced weakening

12   of oceanic circulation (*e.g.,* Delworth and Dixon 2006). Only in the recent decades has

13   the GHG and non-GHG PDI response in these models been in the same direction (Figure

14   5), a constructive influence that is projected to continue over the next few decades

15   (Figure 4).

16   These results add to the growing body of work (*e.g.,* Rotstayn and Lohmann 2002;

17   Mann and Emanuel 2005; Evan *et al.* 2009; Chang *et al.* 2011; Booth *et al.* 2012;

18   Villarini and Vecchi 2012b) suggesting that the observed multi-decadal variability in the

19   North Atlantic, and its related impacts (*e.g.,* the inactive Atlantic hurricane period

20   between the late-1960s and early-1990s), may include a component driven by changes in

21   atmospheric aerosols (primarily through an increase in the post-World War II era, and a

22   decrease in the 1980s-1990s, of aerosol optical depth over the Atlantic). However, the

23   CMIP5 historical experiments only explain a fraction (~25%) of the recently observed

1   multi-decadal swing in PDI (Figure 1), indicating that factors such as internal variability

2   (*e g.,* Zhang and Delworth 2005, 2006, 2009; Robson *et al.* 2012) are also likely to have

3   contributed.

4   In contrast to projections of surface warming, which have already been observed and

5   attributed in part to increasing GHGs (Solomon et al. 2007), for PDI we are in an

6   uncomfortable position where the GCMs are projecting potentially dramatic and

7   societally relevant changes, while at the same time indicating no detectable changes

8   should be present in the record. Therefore, tests of these projections must be indirect and

9   are intimately tied to our confidence in the fidelity of the GCMs and the projected

10   radiative forcing. In particular, because of the role of aerosols changes in the historical

11   simulations and projections of PDI, and because there are currently substantial

12   uncertainties in the role of aerosols in past climate variations (*e.g.,* Booth *et al.* 2012;

13   Zhang *et al.* 2012), efforts should continue to improve our understanding and modeling

14   capability for the role of aerosols in regional and global climate change. More generally,

15   the mechanisms behind patterns of SST must be better understood (*e.g.,* Leloup and

16   Clement 2009; Clement *et al.* 2010; Xie *et al.* 2010), as should the character of past

17   changes in regional SST (*e.g.,* Vecchi and Soden 2007b; Vecchi *et al.* 2008a; Deser *et al.*

18   2010), in order to develop confident projections and assessment of past causes for

19   changes in Atlantic hurricane intensity.

20

10

1   REFERENCES

2   Bender, M.A., T.R. Knutson, R.E. Tuleya, J.J. Sirutis, G.A. Vecchi, S.T. Garner, and I.M.

3   Held, 2010: Model impact of anthropogenic warming on the frequency of intense

4   Atlantic hurricanes. *Science*, **327**, 454–458.

5   Booth, B. B. B., Dunstone, N. J., Halloran, P. R., Andrews, T. & Bellouin, N., 2012:

6   Aerosols implicated as a prime driver of twentieth-century North Atlantic climate

7   variability. *Nature*, **484**, 228-232.

8   Chang, C. Y., Chiang, J. C. H. & Wehner, M. F. Friedman, A. & Ruedy, 2011: R. Sulfate

9   aerosol control of tropical Atlantic climate over the 20th century. *J. Climate*, **24**,

10   2540–2555.

11   Clement, A.C., A.C. Baker, and J. Leloup (2010): Climate Change: Patterns of Tropical

12   Warming. Nature Geoscience 3, 8-9 (2010) doi:10.1038/ngeo728.

13   Delworth, T. L. & Dixon K. W., 2006: Have anthropogenic aerosols delayed a

14   greenhouse gas-induced weakening of the North Atlantic thermohaline circulation?

15   *Geophysical Research Letters*, **33**, L02606, DOI:10.1029/2005GL024980.

16   Deser, C., A. S. Phillips, and M. A. Alexander, 2010: Twentieth century tropical sea

17   surface temperature trends revisited, *Geophys. Res. Lett.*, 37, L10701,

18   doi:10.1029/2010GL043321.

19   Emanuel, K.A., 1987: The dependence of hurricane intensity on climate. *Nature*, **326**,

20   483–485.

21   Emanuel, K. 2005: Increasing destructiveness of tropical cyclones over the past 30 years.

22   *Nature*, **436**, 686–688.

1   Emanuel, K. 2007: Environmental factors affecting tropical cyclone power dissipation.

2   *Journal of Climate*, **20**, 5497-5509.

3   Emanuel, K. 2010: Tropical cyclone activity downscaled from NOAA-CIRES

4   Reanalysis, 1908-1958. *Journal of Advances in Modeling Earth Systems*, **2**, 1-12.

5   Emanuel, K., R. Sundararajan, and J. Williams, 2008: Hurricanes and global warming—

6   Results from downscaling IPCC AR4 simulations. *Bulletin of the American*

7   *Meteorological Society*, **89**, 347–367.

8   Evan, A. T., Vimont, D. J., Heidinger, A. K., Kossin, J. P. & Bennartz, R., 2009: The role

9   of aerosols in the evolution of tropical North Atlantic Ocean temperature anomalies.

10   *Science*, **324**, 778–781.

11   Holland, G.J., 1997: The maximum potential intensity of tropical cyclones. *Journal of*

12   *Atmospheric Sciences*, **54**, 2519–2541.

13   Knutson, T.R., and R.E. Tuleya, 2004: Impact of CO_2-induced warming on simulated

14   hurricane intensity and precipitation: Sensitivity to the choice of climate model and

15   convective parameterization. *Journal of Climate*, **17**, 3477–3495.

16   Knutson, T.R., J.L. McBride, J. chan, K. Emanuel, G. Holland, C. Landsea, I. Held, J.P.

17   Kossin, A.K. Srivastava, and M. Sugi, 2010: Tropical cyclones and climate change.

18   *Nature Geoscience*, **3**, 157–163.

19   Landsea, C.W., 1993: A climatology of intense (or major) Atlantic hurricanes. *Monthly*

20   *Weather Review*, **121**, 1703–1713

21   Latif, M., N. Keenlyside, and J. Bader, 2007: Tropical sea surface temperature, vertical

22   wind shear, and hurricane development. *Geophysical Research Letters*, **34**, L01710,

23   doi:10.1029/2006GL027969.

1   Leloup, J. and A. Clement, 2009: Why is there a minimum in projected warming in the

2   tropical North Atlantic Ocean?, *Geophys. Res. Lett.*, 36, L14802,

3   doi:10.1029/2009GL038609.

4   Mann, M.E., and K.A. Emanuel, 2006: Atlantic hurricane trends linked to climate

5   change. *Eos, Transactions of the American Geophysical Union* **87**,

6   doi:10.1029/2006EO240001.

7   Mendelsohn, R., K. Emanuel, S. Chonabayashi, and L. Bakkensen, 2012: The impact of

8   climate change on global tropical cyclone damage. *Nature Climate Change*, **2**, 205-

9   209.

10   Oouchi, K., J. Yoshimura, H. Yoshimura, R. Mizuta, S. Kusunoki, and A. Noda, 2006:

11   Tropical cyclone climatology in a global warming climate as simulated in a 20-km-

12   mesh global atmospheric model: Frequency and wind intensity analysis. *Journal of*

13   *the Meteorological Society of Japan*, **84**, 259–276.

14   Peduzzi, P., B. Chatenou, H. Dao, A. De Bono, C. Herold, J. Kossin, F. Mouton, and O.

15   Nordbeck, 2012: Global trends in tropical cyclone risk. *Nature Climate Change*, **2**,

16   289-294.

17   Pielke, R.A., J. Gratz, C.W. Landsea, D. Collins, M.A. Saunders, and R. Musulin, 2008:

18   Normalized hurricane damages in the United States: 1900–2005 *Natural Hazards*

19   *Review* **9**, 29–42.

20   R Development Core Team, 2008: *R: A Language and Environment for Statistical*

21   *Computing*. R Foundation for Statistical Computing. [Available online at

22   http://www.R-project.org.]

1 Ramsay, H.A., and A.H. Sobel, 2011: Effects of relative and absolute sea surface

2   temperature on tropical cyclone potential intensity using a single-column model.

3   *Journal of Climate*, **24**, 183–193.

4 Robson, J., Sutton, R., Lohmann, K., Smith, D. & Palmer, M., 2012: Causes of the Rapid

5   Warming of the North Atlantic ocean in the mid 1990s. *J. Climate*. doi:10.1175/JCLI-

6   D-11-00443.1,.

7 Rotstayn, L. D., U Lohmann, 2002: Tropical Rainfall Trends and the Indirect Aerosol

8   Effect. *J. Climate*, **15**, 2103–2116. doi: 10.1175/1520-0442.

9 Smith, T.M., R.W. Reynolds, T.C. Peterson, and J. Lawrimore, 2008: Improvements to

10   NOAA's historical merged land–ocean surface temperature analysis (1880–2006).

11   *Journal of Climate*, **21**, 2283–2296.

12 Sobel, A.H., I.M. Held, and C.S. Bretherton, 2002: The ENSO signal in tropical

13   tropospheric temperature. *Journal of Climate*, **15**, 2702–2706.

14 Solomon, S., and Coauthors, 2007: *Climate change 2007: The physical science basis.*

15   *Contribution of Working Group I to the Fourth Assessment Report of the*

16   *Intergovernmental Panel on Climate* Change. Cambridge University Press,

17   Cambridge, United Kingdom and New York, NY, USA.

18 Stasinopoulos, D.M., R.A. Rigby, and C. Akantziliotou, 2007: gamlss: Generalized

19   Additive Models for Location, Scale and Shape. R Package Version 1.6-0. [Available

20   online at http://cran.r-project.org/web/packages/gamlss/index.html.]

21 Swanson, K.L., 2008: Nonlocality of Atlantic tropical cyclone intensities. *Geochemistry*

22   *Geophysics Geosystems*, **9**, Q04V01, doi:10.1029/2007GC001844

1   Taylor, K.E., R.J. Stouffer, and G.A. Meehl, 2012: An overview of CMIP5 and the

2   experiment design. *Bulletin of the American Meteorological Society*, **93**, 485-498.

3   Vecchi, G.A., and B.J. Soden, 2007a: Effect of remote sea surface temperature change on

4   tropical cyclone potential intensity. *Nature*, **450**, 1066–1071.

5   Vecchi, G.A., and B.J. Soden, 2007b: Global Warming and the Weakening of the

6   Tropical Circulation. *J. Climate*, v20(17), 4316-4340.

7   Vecchi, G.A., A. Clement and B.J. Soden, 2008a: Examining the Tropical Pacific's

8   Response to Global Warming. *EOS, Trans. Amer. Geophys. Union*, v.89(9), pp.81,83.

9   Vecchi, G.A., K.L. Swanson, and B.J. Soden, 2008b: Whither Hurricane Activity?

10   *Science*, **322** (5902), 687-689.

11   Vecchi, G.A., M. Zhao, H. Wang, G. Villarini, A. Rosati, A. Kumar, I.M. Held, and R.

12   Gudgel, 2011: Statistical-dynamical predictions of seasonal North Atlantic hurricane

13   activity. *Monthly Weather Review*, **139**(4), 1070-1082.

14   Villarini, G., and G.A. Vecchi, 2012a: North Atlantic Power Dissipation Index (PDI) and

15   Accumulated Cyclone Energy (ACE): Statistical modeling and sensitivity to sea

16   surface temperature changes. *Journal of Climate*, **25**(2), 625-637.

17   Villarini, G., and G.A. Vecchi, 2012b: Twenty-first-century projections of North Atlantic

18   tropical storms from CMIP5 models. *Nature Climate Change*,

19   doi:10.1038/NCLIMATE1530.

20   Villarini, G., and G.A. Vecchi, 2012c: Multi-season lead forecast of the North Atlantic

21   Power Dissipation Index (PDI) and Accumulated Cyclone Energy (ACE). *Journal of*

22   *Climate* (submitted).

1 Villarini, G., G.A. Vecchi, and J.A. Smith, 2010: Modeling of the dependence of tropical

2   storm counts in the North Atlantic Basin on climate indices. *Monthly Weather*

3   *Review*, **138**(7), 2681–2705.

4 Villarini, G., G.A. Vecchi, T.R. Knutson, M. Zhao, and J.A. Smith, 2011: North Atlantic

5   tropical storm frequency response to anthropogenic forcing: Projections and sources

6   of uncertainty. *Journal of Climate*, **24**(13), 3224-3238.

7 Villarini, G., G.A. Vecchi, and J.A. Smith, 2012: U.S. landfalling and North Atlantic

8   hurricanes: Statistical modeling of their frequencies and ratios. *Monthly Weather*

9   *Review*, **140**, 44–65.

10 Xie, S.P., C. Deser, G.A. Vecchi, J. Ma, H. Teng and A.T. Wittenberg, 2010: Global

11   Warming Pattern Formation: Sea Surface Temperature and Rainfall. *J. Climate.*, 23,

12   966-986. doi: 10.1175/2009JCLI3329.1

13 Zhang, R. and Delworth, T. L., 2005: Simulated tropical response to a substantial

14   weakening of the Atlantic thermohaline circulation. *J. Climate*, **18**,

15   DOI:10.1175/JCLI3460.1.

16 Zhang, R., and T. L. Delworth, 2006: Impact of Atlantic multidecadal oscillations on

17   India/Sahel rainfall and Atlantic hurricanes. *Geophys. Res. Lett.*, **33**, L17712,

18   doi:10.1029/2006GL026267.

19 Zhang, R., and T. L. Delworth, 2009: March: A new method for attributing climate

20   variations over the Atlantic Hurricane Basin's main development region. *Geophysical*

21   *Research Letters*, **36**, L06701, DOI:10.1029/2009GL037260.

22 Zhang, R., and coauthors, 2012: Have aerosols Caused the Observed Atlantic

23   Mutlidecadal Variability? *Science*, submitted.

1   Zhao, M., I.M. Held, and G. A. Vecchi, 2010: Retrospective forecasts of the hurricane

2   season using a global atmospheric model assuming persistence of SST anomalies.

3   *Monthly Weather Review*, **138**, 3858–3868.

4

1   LIST OF TABLES

2

3   TABLE 1. Summary of the 17 global climate models used in this study. For all of them,

4   data for the RCP 2.6, RCP 4.5 and RCP 8.5 are available. The same holds true for the

5    $2 \times CO_2$ runs with the exception of MIROC-ESM-CHEM. The final column indicates the

6   models for which the "greenhouse only" historical experiments were available (see

7   Figure 5).

8

9

2

3   FIG. 1. Time series of PDI anomalies from 1878 to 2099. PDI projections are based on 17

4   GCMs under the CMIP5 for three RCPs. The blue line refers to the observations

5   corrected according to Landsea (1993). The red line represents the median of the model

6   described in Villarini and Vecchi (2012a) fitted to the observations; the orange line

7   represents the median of the reconstructed PDI anomalies based on the statistical model

8   in Villarini and Vecchi (2012a) and using ERSSTv3b SST time series (Smith et al. 2008)

9   as input to the statistical model. The solid black line represents the average of the 17

10   medians from the GCMs. The light (dark) grey areas represent the region between the

11   10th and 90th percentile (minimum and maximum) from the 17 medians. The anomalies

12   are computed with respect to the 1986-2005 period for each model and the observations.

13

14   FIG. 2. Boxplots of the average projected PDI values for three periods (2016-2035, 2046-

15   2065, and 2080-2099) normalized by their values over the 1986-2005 period. Projections

16   are based on 17 GCMs and three RCPs. The whiskers represent the 10th and the 90th

17   percentiles, the limits of the boxes the 25th and 75 percentiles; the horizontal line and

18   square inside the boxes the median and mean, respectively; the horizontal dashes

19   represent the minimum and maximum values. The values of σ indicate the standard

20   deviation out of the 17 GCMs.

21

22   FIG. 3. Top panel: Time series of PDI anomalies for 16 GCMs and $2\times CO_2$ experiment.

23   The solid black line represents the average of the 16 medians from the GCMs. The light

24   (dark) grey areas represent the region between the 10th and 90th percentile (minimum and

25   maximum) from the 16 medians. The dashed black vertical line at year 70 represents the

26   time of CO_2 doubling. The anomalies are computed with respect to the 1986-2005 period

27   for each model. Bottom panel: Slopes of the regression lines for the first 70 years for 16

1 GCMs and $2\times CO_2$ experiment. In the box plots, the dashes represent the minimum and

2 maximum values, the limits of the whiskers represent the 10th and 90th percentiles, the

3 limits of the boxes represent the 25th and 75th percentiles, and the horizontal lines and the

4 squares inside the boxes are the median and the mean, respectively.

5

6 FIG. 4. Plots of the PDI anomalies based on three member ensembles of the GFDL-CM3

7 GCM forced with RCP 4.5 projected $GHG+O_3$ forcing (blue lines) and $GHG+O_3$+aerosol

8 forcing (red/yellow lines). PDI computed using the statistical PDI model of Vecchi and

9 Villarini (2012a). The red line is the three-member ensemble mean, each ensemble

10 member is shown by the orange lines, forced by the full RCP 4.5 projections. The blue

11 lines are from an experiment in which emissions of aerosol precursors over the entire 21st

12 century were held fixed at their 2005 values; light blue lines show the individual

13 ensemble members and the dark blue line shows the ensemble mean.

14

15 FIG. 5. Impact of greenhouse and non-greenhouse forcing on the historical PDI evolution

16 of the CMIP5 models. Time series of the 20-year running average PDI based on the 13

17 CMIP5 global climate models (GCMs) for which a "greenhouse only" historical

18 experiment was available (see Table 1). Shading indicates the ±1 inter-GCM standard

19 deviation for each quantity, lines indicate the 13-model average. Black line and gray

20 shading show the response from the "all forcing" historical experiments (the experiments

21 shown in Figure 1 of the main text). Red shows the response of the "greenhouse only"

22 experiments, in which only greenhouse gases were allowed to change in each experiment.

23 Blue shows the difference of the "all forcing" and "greenhouse only", and gives an

24 indication of the impact of non-greenhouse natural (e.g., solar variations and volcanoes)

25 and anthropogenic (e.g., tropospheric aerosols, ozone) forcing agents.

26

1   FIG. 6. Time series of the number of GCMs with median PDI anomaly exceeding that of

2   the year 2005 (3.63 10^{11} m^3 s^{-2}, based on the observations) for three RCPs. The anomalies

3   are computed with respect to the 1986-2005 period for each model and the observations.

4

1 TABLE 1. Summary of the 17 global climate models used in this study. For all of them,

2 data for the RCP 2.6, RCP 4.5 and RCP 8.5 are available. The same holds true for the

3 2×CO₂ runs with the exception of MIROC-ESM-CHEM. The final column indicates the

4 models for which the "greenhouse only" historical experiments were available (see

5 Figure 5).

6

Modeling Center (or Group)	Model Name	Historical	RCP 2.6	RCP 4.5	RCP 8.5	2×CO₂	GHG-only
Beijing Climate Center, China Meteorological Administration	BCC-CSM1.1	Y	Y	Y	Y	Y	Y
Canadian Centre for Climate Modelling and Analysis	CanESM2	Y	Y	Y	Y	Y	Y
National Center for Atmospheric Research	CCSM4	Y	Y	Y	Y	Y	Y
Centre National de Recherches Meteorologiques / Centre Europeen de Recherche et Formation Avancees en Calcul Scientifique	CNRM-CM5	Y	Y	Y	Y	Y	Y
Commonwealth Scientific and Industrial Research Organization in collaboration with Queensland Climate Change Centre of Excellence	CSIRO-Mk3.6.0	Y	Y	Y	Y	Y	Y
NOAA Geophysical Fluid Dynamics Laboratory	GFDL-CM3	Y	Y	Y	Y	Y	Y
NOAA Geophysical Fluid Dynamics Laboratory	GFDL-ESM2M	Y	Y	Y	Y	Y	Y
NOAA Geophysical Fluid Dynamics Laboratory	GFDL-ESM2G	Y	Y	Y	Y	Y	-
Met Office Hadley Centre	HadGEM2-ES	Y	Y	Y	Y	Y	Y
Institut Pierre-Simon Laplace	IPSL-CM5A-LR	Y	Y	Y	Y	Y	Y
Institut Pierre-Simon Laplace	IPSL-CM5A-MR	Y	Y	Y	Y	Y	-
Atmosphere and Ocean Research Institute (The University of Tokyo), National Institute for	MIROC5	Y	Y	Y	Y	Y	-

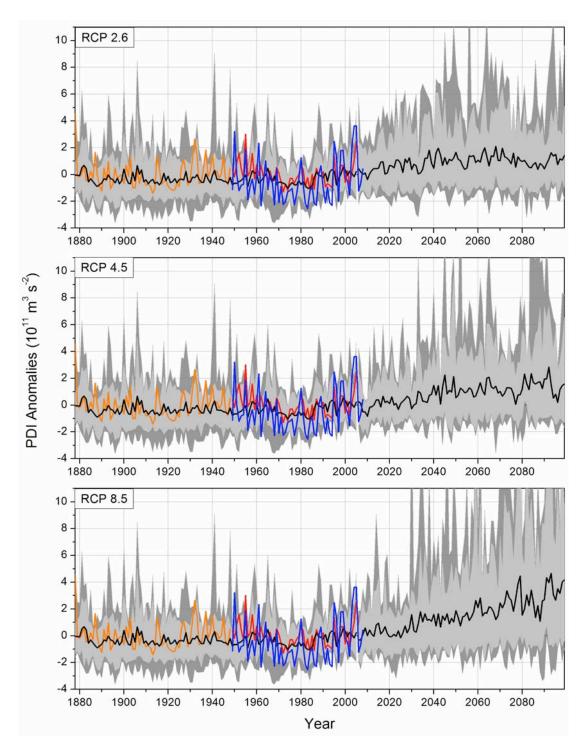|							
Environmental Studies, and Japan Agency for Marine-Earth Science and Technology							
Japan Agency for Marine-Earth Science and Technology, Atmosphere and Ocean Research Institute (The University of Tokyo), and National Institute for Environmental Studies	MIROC-ESM	Y	Y	Y	Y	Y	Y
Japan Agency for Marine-Earth Science and Technology, Atmosphere and Ocean Research Institute (The University of Tokyo), and National Institute for Environmental Studies	MIROC-ESM-CHEM	Y	Y	Y	Y	-	Y
Max Planck Institute for Meteorology	MPI-ESM-LR	Y	Y	Y	Y	Y	-
Meteorological Research Institute	MRI-CGCM3	Y	Y	Y	Y	Y	Y
Norwegian Climate Centre	NorESM1-M	Y	Y	Y	Y	Y	Y

1
2

3

1

2   FIG. 1. Time series of PDI anomalies from 1878 to 2099. PDI projections are based on 17

3   GCMs under the CMIP5 for three RCPs. The blue line refers to the observations

4   corrected according to Landsea (1993). The red line represents the median of the model

5   described in Villarini and Vecchi (2012a) fitted to the observations; the orange line

6   represents the median of the reconstructed PDI anomalies based on the statistical model

1   in Villarini and Vecchi (2012a) and using ERSSTv3b SST time series (Smith et al. 2008)

2   as input to the statistical model. The solid black line represents the average of the 17

3   medians from the GCMs. The light (dark) grey areas represent the region between the

4   10th and 90th percentile (minimum and maximum) from the 17 medians. The anomalies

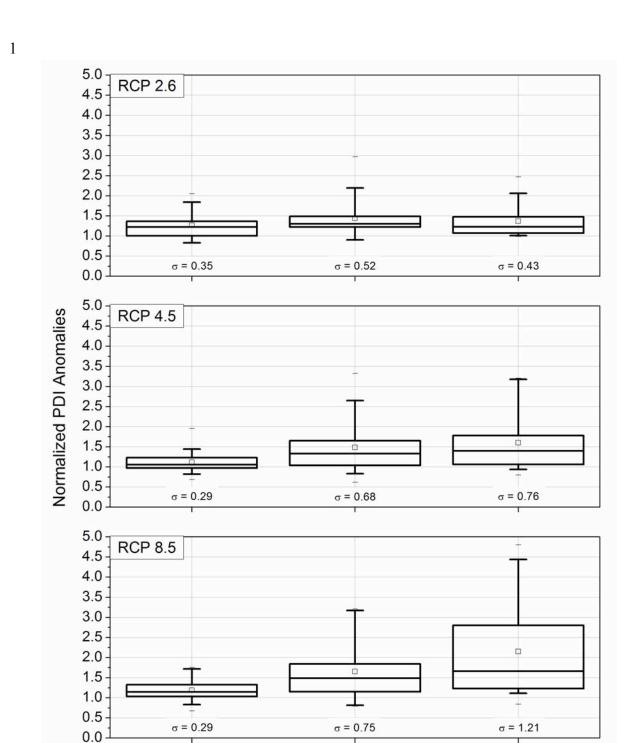5   are computed with respect to the 1986-2005 period for each model and the observations.

6

1

2

3 FIG. 2. Boxplots of the average projected PDI values for three periods (2016-2035, 2046-

4 2065, and 2080-2099) normalized by their values over the 1986-2005 period. Projections

5 are based on 17 GCMs and three RCPs. The whiskers represent the 10th and the 90th

1   percentiles, the limits of the boxes the 25th and 75 percentiles; the horizontal line and

2   square inside the boxes the median and mean, respectively; the horizontal dashes

3   represent the minimum and maximum values. The values of σ indicate the standard

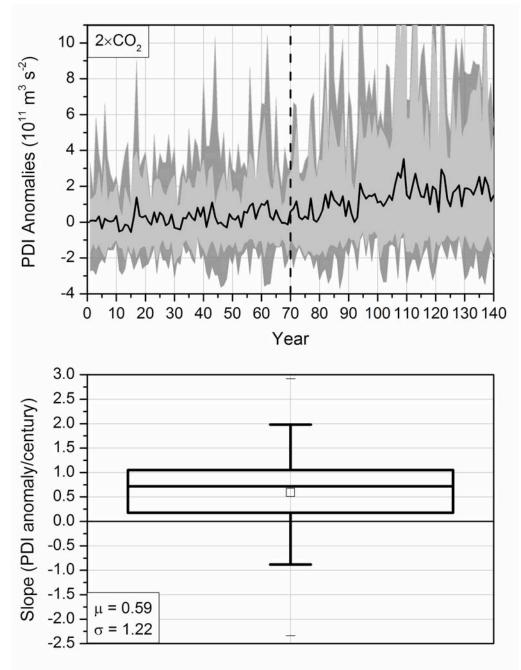4   deviation out of the 17 GCMs.

5

1

2

3   FIG. 3. Top panel: Time series of PDI anomalies for 16 GCMs and $2\times CO_2$ experiment.

4   The solid black line represents the average of the 16 medians from the GCMs. The light

5   (dark) grey areas represent the region between the 10th and 90th percentile (minimum and

6   maximum) from the 16 medians. The dashed black vertical line at year 70 represents the

7   time of CO_2 doubling. The anomalies are computed with respect to the 1986-2005 period

8   for each model. Bottom panel: Slopes of the regression lines for the first 70 years for 16

1   GCMs and $2\times CO_2$ experiment. In the box plots, the dashes represent the minimum and

2   maximum values, the limits of the whiskers represent the 10th and 90th percentiles, the

3   limits of the boxes represent the 25th and 75th percentiles, and the horizontal lines and the

4   squares inside the boxes are the median and the mean, respectively.
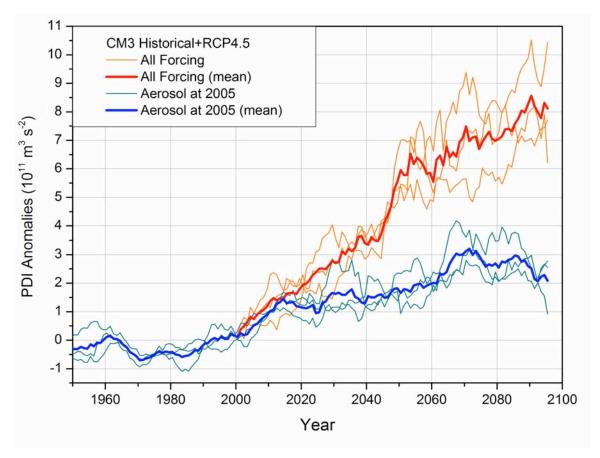
5

6

1

2

3   FIG. 4. Plots of the PDI anomalies based on three member ensembles of the GFDL-CM3

4   GCM forced with RCP 4.5 projected GHG+O_3 forcing (blue lines) and GHG+O_3+aerosol

5   forcing (red/yellow lines). PDI computed using the statistical PDI model of Vecchi and

6   Villarini (2012a). The red line is the three-member ensemble mean, each ensemble

7   member is shown by the orange lines, forced by the full RCP 4.5 projections. The blue

8   lines are from an experiment in which emissions of aerosol precursors over the entire 21st

9   century were held fixed at their 2005 values; light blue lines show the individual

10   ensemble members and the dark blue line shows the ensemble mean.

11
12

CMIP5 Historical Simulations

All Forcing   Greenhouse-only   All minus GHG
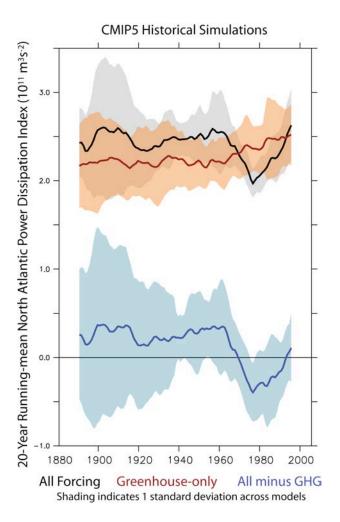Shading indicates 1 standard deviation across models

1
2
3   FIG. 5. Impact of greenhouse and non-greenhouse forcing on the historical PDI evolution
4   of the CMIP5 models. Time series of the 20-year running average PDI based on the 13
5   CMIP5 global climate models (GCMs) for which a "greenhouse only" historical
6   experiment was available (see Table 1). Shading indicates the ±1 inter-GCM standard
7   deviation for each quantity, lines indicate the 13-model average. Black line and gray
8   shading show the response from the "all forcing" historical experiments (the experiments
9   shown in Figure 1 of the main text). Red shows the response of the "greenhouse only"
10   experiments, in which only greenhouse gases were allowed to change in each experiment.
11   Blue shows the difference of the "all forcing" and "greenhouse only", and gives an
12   indication of the impact of non-greenhouse natural (e.g., solar variations and volcanoes)
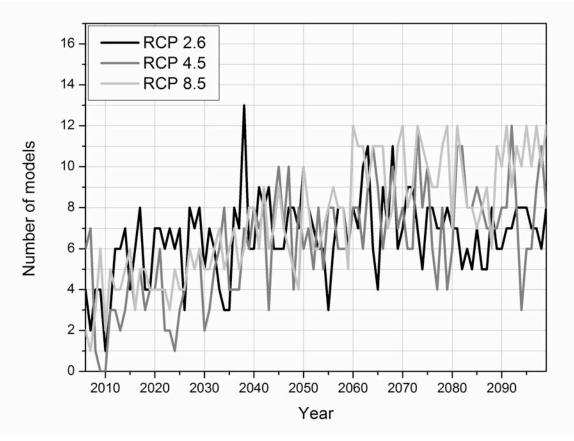13   and anthropogenic (e.g., tropospheric aerosols, ozone) forcing agents.
14

1
2

3
4 FIG. 6. Time series of the number of GCMs with median PDI anomaly exceeding that of
5 the year 2005 (3.63 10^{11} m^3 s^{-2}, based on the observations) for three RCPs. The anomalies
6 are computed with respect to the 1986-2005 period for each model and the observations.
7
8
9
10